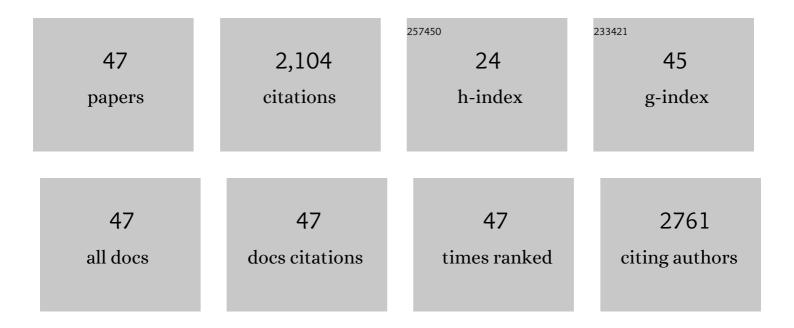
Lei Zhang

List of Publications by Year in descending order

Source: https://exaly.com/author-pdf/1237118/publications.pdf Version: 2024-02-01



#	Article	IF	CITATIONS
1	Interfacial electronic modification of bimetallic oxyphosphides as Multi-functional electrocatalyst for water splitting and urea electrolysis. Journal of Colloid and Interface Science, 2022, 607, 546-555.	9.4	26
2	In-situ fabrication of 3D hierarchical flower-like β-Bi2O3@CoO Z-scheme heterojunction for visible-driven simultaneous degradation of multi-pollutants. Journal of Hazardous Materials, 2021, 403, 123566.	12.4	49
3	In situ confine of Co3ZnC/Co in N-doped carbon nanotube-grafted graphitic carbon nanoflakes as 1D-2D hierarchical catalysts toward superior redox activity. Applied Catalysis B: Environmental, 2021, 281, 119513.	20.2	46
4	Designed Tb(III)-Functionalized MOF-808 as Visible Fluorescent Probes for Monitoring Bilirubin and Identifying Fingerprints. Inorganic Chemistry, 2021, 60, 3172-3180.	4.0	48
5	Fabricating multifunctional low-toxicity ratiometric fluorescent probe for individual detection of Cu2+/glutamate and continuous sensing for glutamate via Cu2+-based platform. Spectrochimica Acta - Part A: Molecular and Biomolecular Spectroscopy, 2021, 259, 119892.	3.9	14
6	Facile fabrication of 3D hierarchical micro-nanostructure fluorine-free superhydrophobic materials by a simple and low-cost method for efficient separation of oil-water mixture and emulsion. Journal of Environmental Chemical Engineering, 2021, 9, 106400.	6.7	9
7	Construction of 3D Bi/ZnSnO ₃ hollow microspheres for label-free highly selective photoelectrochemical recognition of norepinephrine. Nanoscale, 2021, 13, 9270-9279.	5.6	8
8	3D hierarchical hollow microrod via in-situ growth 2D SnS nanoplates on MOF derived Co, N co-doped carbon rod for electrochemical sensing. Sensors and Actuators B: Chemical, 2020, 303, 127208.	7.8	21
9	Tailorable yolk-shell Fe3O4@graphitic carbon submicroboxes as efficient extraction materials for highly sensitive determination of trace sulfonamides in food samples. Food Chemistry, 2020, 303, 125369.	8.2	58
10	A dual mode photoelectrochemical sensor for nitrobenzene and L-cysteine based on 3D flower-like Cu2SnS3@SnS2 double interfacial heterojunction photoelectrode. Journal of Hazardous Materials, 2020, 382, 121026.	12.4	23
11	Assembling 3D hierarchical hollow flower-like Ni@N-doped graphitic carbon for boosting simultaneously efficient removal and sensitive monitoring of multiple sulfonamides. Journal of Hazardous Materials, 2020, 386, 121629.	12.4	23
12	Fabrication of Dandelion-like p–p Type Heterostructure of Ag ₂ 0@CoO for Bifunctional Photoelectrocatalytic Performance. Langmuir, 2020, 36, 12357-12365.	3.5	17
13	Fabricated smart sponge with switchable wettability and photocatalytic response for controllable oil-water separation and pollutants removal. Journal of Industrial and Engineering Chemistry, 2020, 92, 278-286.	5.8	26
14	Z-Scheme 2D/3D hierarchical MoS ₂ @CoMoS ₄ flower-shaped arrays with enhanced full spectrum light photoelectrocatalytic activity for H ₂ O ₂ / <i>p</i> -aminophenol production and contaminant degradation. Journal of Materials Chemistry A, 2020, 8, 25890-25903.	10.3	19
15	An <i>in situ</i> engineered CuCo ₂ S ₄ @CuCo ₂ O ₄ heterojunction with an O–S interpenetrated interface as a photoanode for selective photoelectrochemical bioanalysis. Journal of Materials Chemistry A, 2020, 8, 9077-9084.	10.3	14
16	N-enriched porous carbon encapsulated bimetallic phosphides with hierarchical structure derived from controlled electrodepositing multilayer ZIFs for electrochemical overall water splitting. Applied Catalysis B: Environmental, 2019, 259, 118053.	20.2	72
17	3D pothole-rich hierarchical carbon framework-encapsulated Ni nanoparticles for highly selective nonenzymatic cysteine detection. Electrochimica Acta, 2019, 328, 135126.	5.2	12
18	Fast Coadsorption and Selective Separation of Gallium(III) and Germanium(IV) from Aqueous Solutions by 3D Hierarchical Porous Hoya-like α-FeOOH. ACS Sustainable Chemistry and Engineering, 2019, 7, 15939-15947.	6.7	26

Lei Zhang

#	Article	IF	CITATIONS
19	Architecting Z-scheme Bi2S3@CoO with 3D chrysanthemums-like architecture for both photoeletro-oxidization and -reduction performance under visible light. Chemical Engineering Journal, 2019, 378, 122092.	12.7	48
20	Construction of magnetic core-ring-structured porous hexagonal NiCo2O4 nanoplates/carbon fibers hybrid with enhanced visible-light photocatalytic performance. Journal of Materials Science, 2019, 54, 7617-7627.	3.7	5
21	Fabrication of Ecofriendly Recycled Marimo-like Hierarchical Micronanostructure Superhydrophobic Materials for Effective and Selective Separation of Oily Pollutants from Water. Industrial & Engineering Chemistry Research, 2019, 58, 5613-5621.	3.7	14
22	Fabrication of Porous Zirconia Microspheres as an Efficient Adsorbent for Removal and Recovery of Trace Se(IV) and Te(IV). Industrial & Engineering Chemistry Research, 2019, 58, 342-349.	3.7	21
23	Insight into the energy band alignment of magnetically separable Ag2O/ZnFe2O4 p-n heterostructure with rapid charge transfer assisted visible light photocatalysis. Journal of Catalysis, 2019, 370, 289-303.	6.2	165
24	Rational design and fabrication of multifunctional catalyzer Co2SnO4-SnO2/GC for catalysis applications: Photocatalytic degradation/catalytic reduction of organic pollutants. Applied Catalysis B: Environmental, 2018, 231, 34-42.	20.2	56
25	Bubble-supported engineering of hierarchical CuCo ₂ S ₄ hollow spheres for enhanced electrochemical performance. Journal of Materials Chemistry A, 2018, 6, 5265-5270.	10.3	103
26	3D hierarchical magnetic hollow sphere-like CuFe2O4 combined with HPLC for the simultaneous determination of Sudan l–IV dyes in preserved bean curd. Food Chemistry, 2018, 241, 268-274.	8.2	54
27	Fabrication of 3D Hierarchical Byttneria Aspera‣ike Ni@Graphitic Carbon Yolk–Shell Microspheres as Bifunctional Catalysts for Ultraefficient Oxidation/Reduction of Organic Contaminants. Small, 2018, 14, e1803188.	10.0	32
28	A magnetic cellulose-based carbon fiber hybrid as a dispersive solid-phase extraction material for the simultaneous detection of six bisphenol analogs from environmental samples. Analyst, The, 2018, 143, 3100-3106.	3.5	26
29	Simultaneous Electrochemical Detection of Benzimidazole Fungicides Carbendazim and Thiabendazole Using a Novel Nanohybrid Material-Modified Electrode. Journal of Agricultural and Food Chemistry, 2017, 65, 727-736.	5.2	113
30	Controlled synthesis of hollow porous carbon spheres for enrichment and simultaneous determination of nine bisphenols from real samples. Talanta, 2017, 167, 428-435.	5.5	20
31	Design and construction of a bifunctional magnetically recyclable 3D CoMn ₂ O ₄ /CF hybrid as an adsorptive photocatalyst for the effective removal of contaminants. Physical Chemistry Chemical Physics, 2017, 19, 25044-25051.	2.8	15
32	Fabrication of Octahedral Cu@Graphitic Carbon Cage Complex Porous Structures and Their Microwave-Driven Catalytic Activity. ACS Sustainable Chemistry and Engineering, 2017, 5, 7800-7811.	6.7	13
33	Fabrication of 3D hierarchical CoSnO ₃ @CoO pine needle-like array photoelectrode for enhanced photoelectrochemical properties. Journal of Materials Chemistry A, 2017, 5, 18664-18673.	10.3	46
34	Waxberry-like magnetic porous carbon composites prepared from a nickel-organic framework for solid-phase extraction of fluoroquinolones. Mikrochimica Acta, 2017, 184, 4107-4115.	5.0	47
35	Magnetic solid-phase extraction using nanoporous three dimensional graphene hybrid materials for high-capacity enrichment and simultaneous detection of nine bisphenol analogs from water sample. Journal of Chromatography A, 2016, 1463, 1-10.	3.7	56
36	Functionalization of magnetic hollow porous oval shape NiFe2O4 as a highly selective sorbent for the simultaneous determination of five heavy metals in real samples. Talanta, 2016, 161, 288-296.	5.5	30

Lei Zhang

#	Article	IF	CITATIONS
37	Superior performance of 3 D Co-Ni bimetallic oxides for catalytic degradation of organic dye: Investigation on the effect of catalyst morphology and catalytic mechanism. Applied Catalysis B: Environmental, 2016, 186, 193-203.	20.2	74
38	New approach for the simultaneous determination fungicide residues in food samples by using carbon nanofiber packed microcolumn coupled with HPLC. Food Control, 2016, 60, 1-6.	5.5	29
39	An Electrochemical Method for High Sensitive Detection of Thiabendazole and Its Interaction with Human Serum Albumin. Food Analytical Methods, 2015, 8, 507-514.	2.6	21
40	One-Step Fabrication of a Multifunctional Magnetic Nickel Ferrite/Multi-walled Carbon Nanotubes Nanohybrid-Modified Electrode for the Determination of Benomyl in Food. Journal of Agricultural and Food Chemistry, 2015, 63, 4746-4753.	5.2	14
41	The investigation of synergistic and competitive interaction between dye Congo red and methyl blue on magnetic MnFe2O4. Chemical Engineering Journal, 2014, 246, 88-96.	12.7	158
42	New Approach for Highly Selective Separation and Recovery of Osmium and Rhodium by Using a Nanoparticle Microcolumn. Industrial & Engineering Chemistry Research, 2014, 53, 15200-15206.	3.7	6
43	Sorption behavior of germanium(IV) on titanium dioxide nanoparticles. Russian Journal of Inorganic Chemistry, 2012, 57, 622-628.	1.3	6
44	Separation of trace amounts of Ga and Ge in aqueous solution using nano-particles micro-column. Talanta, 2011, 85, 2463-2469.	5.5	18
45	Studies on the removal of tetracycline by multi-walled carbon nanotubes. Chemical Engineering Journal, 2011, 178, 26-33.	12.7	338
46	Kinetic and thermodynamic studies of adsorption of gallium(III) on nano-TiO2. Rare Metals, 2010, 29, 16-20.	7.1	34
47	Sorption characteristics and separation of tellurium ions from aqueous solutions using nano-TiO2. Talanta, 2010, 83, 344-350.	5.5	31